ARTICLE

Graphene Oxide Papers Modified by Divalent Ions—Enhancing Mechanical Properties *via* Chemical Cross-Linking

Sungjin Park,[†] Kyoung-Seok Lee,[‡] Gulay Bozoklu,[§] Weiwei Cai,[⊥] SonBinh T. Nguyen,[∥,*] and Rodney S. Ruoff[†,#,*]

[†]Department of Mechanical Engineering, Northwestern University, 2145 Sheridan Road, Evanston, Illinois 60208-3111, [‡]Korea Research Institute of Standard and Science, 1 Doryong-Dong, Yuseong-Gu, Daejeon, Republic of Korea, [§]Faculty of Engineering and Natural Science, Sabanci University, Orhanli Tuzla 34956, Istanbul, Turkey, [⊥]Beijing National Laboratory for Condensed Matter Physics, Institute of Physics, Chinese Academy of Science, China, and [∥]Department of Chemistry, Northwestern University, 2145 Sheridan Road, Evanston, Illinois 60208-3111. [#]Present address: Department of Mechanical Engineering, University of Texas at Austin, One University Station C2200, Austin, TX 78712-0292.

ABSTRACT Significant enhancement in mechanical stiffness (10–200%) and fracture strength (~50%) of graphene oxide paper, a novel paperlike material made from individual graphene oxide sheets, can be achieved upon modification with a small amount (less than 1 wt %) of Mg^{2+} and Ca^{2+}. These results can be readily rationalized in terms of the chemical interactions between the functional groups of the graphene oxide sheets and the divalent metals ions. While oxygen functional groups on the basal planes of the sheets and the carboxylate groups on the edges can both bond to Mg^{2+} and Ca^{2+}, the main contribution to mechanical enhancement of the paper comes from the latter.

KEYWORDS: graphene oxide · graphene oxide paper · graphite · divalent ion · cross-linking · mechanical property

Over the past decade, graphene-based chemistry, physics, and materials have attracted significant attention[1–8] because of the excellent mechanical and electrical properties that the graphene sheet was predicted to possess. Among known strategies for generating graphene-based materials, the modification of graphite oxide (GO), generated by oxidation of graphite,[9] is arguably the most versatile and easily scalable method. Notably, the wide range of oxygen functional groups on both basal planes and edges of GO[10–13] allows it to be readily exfoliated and functionalized to yield well-dispersed solutions of individual graphene oxide sheets in both water[14] and organic solvents,[15] providing more possibilities for applications in materials science and nanocomposites.[16–18] Graphene oxide sheets have also been used in the flow-directed fabrication of graphene oxide paper,[19] a novel free-standing paperlike material with good mechanical properties. Herein, we report significant enhancements in the mechanical properties of graphene oxide paper upon modification with a small amount of divalent alkaline earth metal ions (Mg^{2+} and Ca^{2+}). These results can be readily rationalized in terms of the chemical interactions between the functional groups of the graphene oxide sheets and the divalent metals ions.

As a versatile starting material, graphene oxide sheets can be readily manipulated *via* chemical functionalization. For example, a highly conductive nanocomposite of polystyrene with uniformly dispersed graphene sheets was obtained by the reduction of isocyanate-functionalized graphene oxide in the presence of the polymer.[16] In addition, transparent and electrically conductive ceramic composites of graphene-based sheets were produced by exposure of silica sol–gels containing well-dispersed graphene oxide sheets to hydrazine vapor that condensed on the sol–gel surface, prior to final curing.[18] Given these promising initial developments, we have continued to explore new chemistry and material applications based on graphene oxide sheets. In particular, because graphene ox-

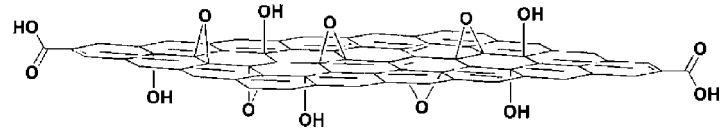

Figure 1. Schematic model of a sheet of graphene oxide showing possible oxygen-containing functionalities

*Address correspondence to r.ruoff@mail.texas.edu, stn@northwestern.edu.

Received for review November 5, 2007 and accepted February 12, 2008.

Published online March 6, 2008. 10.1021/nn700349a CCC: $40.75

ide sheets are known to possess reactive carboxylic acid and hydroxyl moieties (Figure 1),[10–13] we further hypothesized that chemically cross-linking these functionalities could significantly enhance the overall mechanical properties of macroscopic graphene oxide paper samples. To this end, we have employed Mg^{2+} and Ca^{2+} as the cross-linkers due to their well-known ability to bind readily to oxygen functional groups.

While aqueous suspensions of graphene oxide remain stable in the presence of alkali metal salts such as LiCl and NaCl (see Supporting Information (SI)), addition of alkaline-earth MCl_2 salts (M = Mg and Ca) immediately led to agglomeration of the sheets and uncontrollable precipitation, presumably due to the cross-linking of the graphene oxide sheets by the divalent cations. Consequently, we decided to employ premade graphene oxide paper as the starting point for metal-ion-modification by passing an aqueous solution of MCl_2 through a wet membrane of graphene oxide paper under suction (continuous filtration method) (see SI). As the total amount of metal ions used during this process is in excess of the available oxygen functionalities (see SI), it is possible that unbound or weakly bound metal ions may be present in the gallery regions between graphene oxide sheets and this may affect the mechanical properties of the as-prepared paper. Consequently, we also prepared a separate set of rinsed M-modified graphene oxide paper by passing deionized water through samples of wet as-prepared M-modified graphene oxide paper. SEM images of the fracture edges of both types of M-modified graphene oxide papers clearly showed the maintenance of the well-stacked layer structure of the parent graphene oxide paper (see SI).

Tensile testing of graphene oxide papers that were modified with Mg^{2+} and Ca^{2+}, both as-prepared and rinsed, revealed uniformly high values of modulus and tensile strength but with distinct modulus-change profiles (Figure 2). Similar to unmodified graphene oxide paper, the stress–strain curves of M-modified samples also exhibited an initial straightening region followed by a "linear region" (see discussion in ref 19 that explains that this region, although almost linear, is not perfectly elastic for unmodified graphene oxide paper and is thus referred to as the "linear region" here), each with consistently increasing moduli (Figure 2a,b). Suspecting that the level of metal modification—particularly the different types of chemical bonds between the metal ions and the graphene oxide sheets (see later)—could result in significant changes in mechanical behaviors of the graphene oxide paper at different strain scales, we examined the moduli for all samples in the initial, straightening, and linear region of the stress–strain curves.

The initial moduli (E_I) of M-modified samples are 70–200% higher than that for unmodified graphene oxide paper, indicating that M-modified papers are significantly stiffer than the unmodified paper against initial loading (Table 1). These moduli continue to increase as the samples straighten and enter the linear region, albeit at a different rate. The moduli (E_S) of the M-modified samples during straightening—proposed to involve the structural sliding of the graphene oxide sheets to overcome any physical wrinkling that results from the fabrication of the paper and thus to achieve the best interlocking geometry[19]—are uniformly 30–40% higher than that for the unmodified paper except for the as-prepared Ca-modified sample, which shows similar E_S as that for the unmodified paper.

In the linear region, the rinsed M-modified papers are ~10% stiffer than the unmodified paper (Table 1). These moduli (E_E) are much higher than reported moduli values for bucky paper (<10 GPa),[20] graphite foil (~5 GPa),[21] and paperlike materials (~14 GPa).[22] Interestingly, the rinsed M-modified papers are much stiffer than the corresponding as-prepared M-modified papers, with a relative enhancement of 13% for M = Mg and 31% for M = Ca. Significantly, the fracture strength (σ) of the rinsed Ca-modified graphene oxide paper was 54% higher than that of the unmodified graphene oxide paper and 67% higher than that for the as-prepared Ca-modified analogue. Most importantly, these increases in stiffness and strengths did not negatively impact the native toughness of the graphene oxide paper—the ultimate strains (ϵ) of both as-prepared and rinsed M-modified papers are similar to that for the unmodified paper.

The X-ray diffraction (XRD) patterns of the M-modified graphene oxide paper (Figure 3a and see SI) showed an increased layer-to-layer distance (*d*-spacing) compared to that of the unmodified graphene oxide paper. While the XRD peak of the unmodified graphene oxide paper showed a *d*-spacing ≈ 0.83 nm,[23] those for the Mg- and Ca-modified graphene oxide shifted to lower θ values, which is strong evidence of the intercalation of these metal ions (Mg^{2+} has an ionic radius of 0.078 nm and Ca^{2+} an ionic radius of 0.106 nm)[24] into the gallery spaces between the graphene oxide sheet basal planes. Inductively coupled plasma mass spectrometric (ICP−MS) analysis of Mg-modified graphene oxide papers (see SI) showed a significant metal content (12 ppm by weight) that is greatly reduced (to 5 ppm by weight, respectively) after rinsing. Furthermore, the *d*-spacing of the Mg- and Ca-modified graphene oxide papers both decreased to that for the unmodified graphene oxide paper after rinsing, indicating significant reduction in the amount of incorporated metal ions (see SI). Given the expected chemical functionalities that are present on graphene oxide sheets,[10–13] these data suggest two modes of interactions for alkaline earth metal ions with the graphene oxide sheets in our M-modified paper (Figure 4a): (1) bridging the edges of the sheets through carboxylate chelates to the metal and (2) intercalating between the basal planes through either weak alkoxide or dative bonds

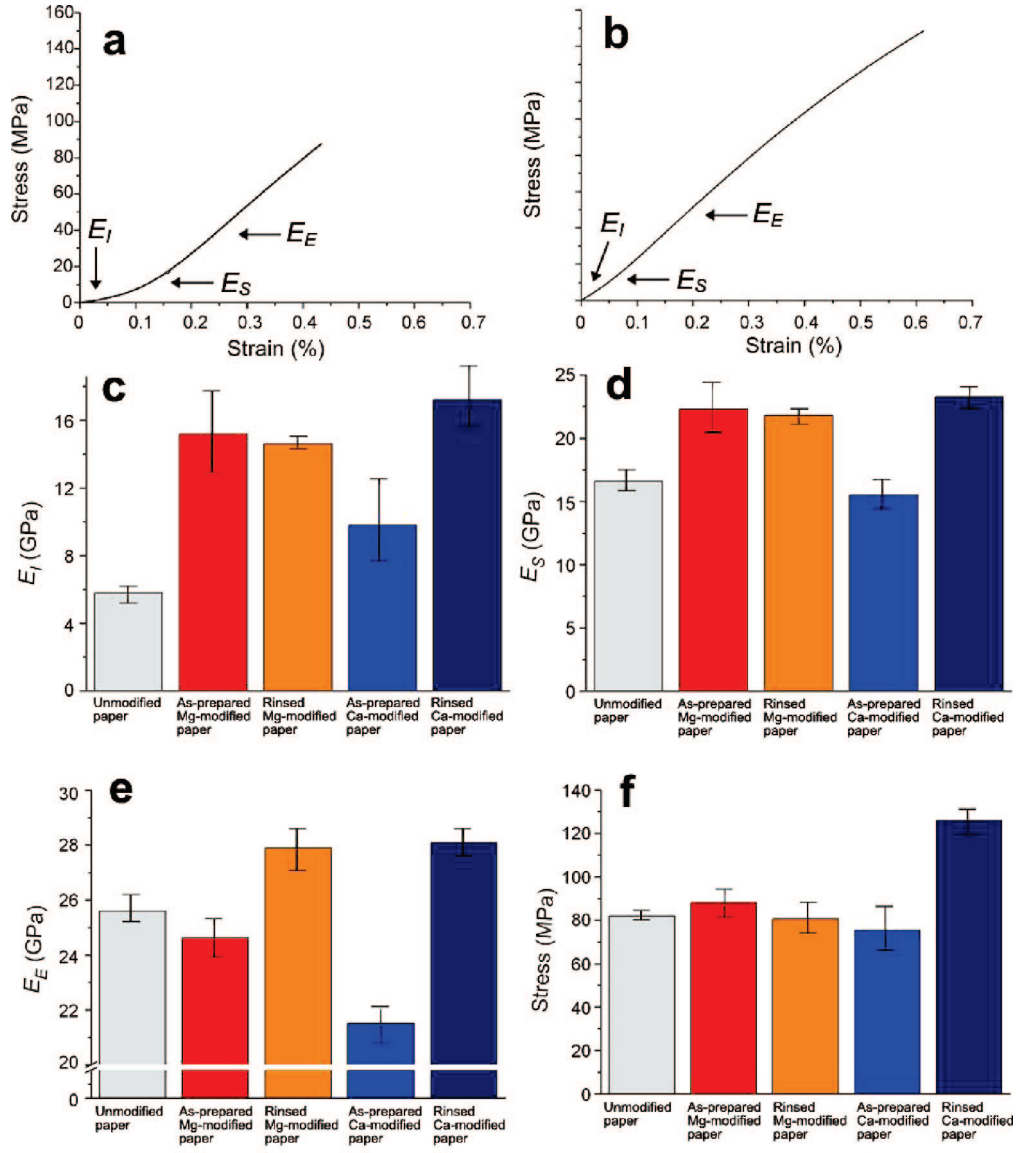

Figure 2. Mechanical data and properties of unmodified and M-modified graphene oxide papers: (a) stress–strain curve of unmodified graphene oxide paper from tensile testing; (b) stress–strain curve of rinsed Ca-modified graphene oxide paper from tensile testing; (c) graphical comparison of the initial moduli (E_I) of both unmodified and M-modified graphene oxide papers; (d) graphical comparison of the moduli in the straightening region (E_S); (e) graphical comparison of the moduli in the linear region (E_E); (f) graphical comparison of the ultimate stress (σ).

from carbonyl and hydroxyl groups. While the former bonding mode is strong, the latter interactions are weak and can be removed by water rinsing.[24]

Energy dispersive X-ray (EDX) fluorescent mapping of the cross-section of the M-modified graphene oxide papers, as-prepared and after rinsing, revealed overall homogeneous distributions of alkaline earth ions across the thickness of the samples (see SI) and verified that our continuous filtration method did not lead to inhomogeneities in the sample. Consistent with the ICP−MS data (see above), the overall level of metal ions decreased upon rinsing.

TABLE 1. Mechanical Properties of Unmodified and M-Modified Graphene Oxide Papers[a]

materials	E_I (GPa)	E_S (GPa)	E_E (GPa)	σ (Mpa)	ϵ (%)
unmodified paper	5.8 ± 1.4	16.6 ± 2.2	25.6 ± 1.1	81.9 ± 5.3	0.40 ± 0.03
as-prepared Mg-modified paper	15.2 ± 4.6	22.3 ± 3.1	24.6 ± 1.4	87.9 ± 14.2	0.40 ± 0.04
rinsed Mg-modified paper	14.6 ± 0.3	21.8 ± 1.5	27.9 ± 1.8	80.6 ± 16.5	0.33 ± 0.08
as-prepared Ca-modified paper	9.8 ± 4.5	15.5 ± 2.4	21.5 ± 1.5	75.4 ± 21.6	0.41 ± 0.15
rinsed Ca-modified paper	17.2 ± 3.4	23.3 ± 1.8	28.1 ± 1.2	125.8 ± 13.6	0.50 ± 0.06

[a] E_I = modulus in the initial region where loading is started; E_S = modulus at σ = 10 MPa in the straightening region; E_E = maximum modulus in the linear region.

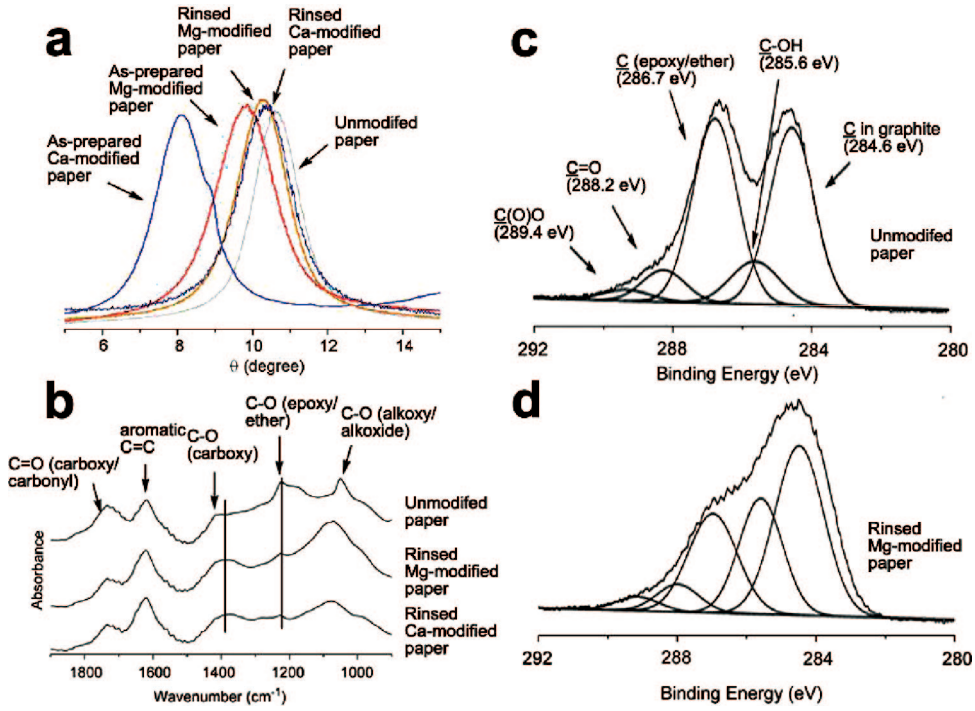

Figure 3. X-ray and spectroscopic analysis of unmodified and M-modified graphene oxide papers: (a) XRD patterns; (b) FT-IR spectra; (c) deconvoluted XPS spectrum of the unmodified graphene oxide paper in the C1*s* region; (d) deconvoluted XPS spectrum of the rinsed Mg-modified graphene oxide paper in the C1*s* region.

The Fourier-transformed infrared spectra of rinsed M-modified graphene oxide papers all showed C═O, aromatic C═C, carboxy C−O, epoxy/ether C−O, and alkoxy/alkoxide C−O stretches (Figure 3b and see SI).[25] In comparison to the IR spectrum of graphene oxide paper, those for rinsed M-modified graphene oxide papers exhibited decreased C═O stretch intensities as well as increased carboxy C−O stretch intensities whose peak positions are also shifted to lower wavenumbers. This is typically interpreted as evidence for carboxylic acid coordinates to a divalent metal ion,[26] which can potentially lead to cross-links between individual graphene oxide sheets in the M-modified paper. Notably, the relative intensity of the epoxy/ether C−O stretch at 1222 cm^{-1} significantly decreased after exposure of graphene oxide paper to the MCl_2 salt solutions and rinsing. As graphene oxide has been suggested to contain reactive epoxy groups,[10–13] its exposure to Lewis acidic divalent metal ions such as M^{2+} may have led to ring-opening of the epoxide (see SI). Consistent with this interpretation, the reduction of the relative intensity of the epoxy/ether stretch accompanies a simultaneous increase of the relative intensity of the stretch at 1100 cm^{-1}, which corresponds to hydroxyl and alkoxide C−O stretches.

Additional support for the possibility that new types of C−O bonds may result from epoxide ring-opening comes from X-ray photoelectron spectroscopy (XPS). In contrast to unmodified graphene oxide paper, the C1*s* XPS spectrum for Mg-modified graphene oxide paper (Figure 3c,d) shows a significantly decreased component for the C of the epoxy/ether group (286.7 eV) and an increased component for the hydroxyl/alkoxide C,[27] supporting the hypothesis that alcohol groups are generated by the ring-opening reaction of epoxides. The C1*s* component corresponding to carboxylic acid groups was slightly shifted from 289.4 to 289.1 eV, indicative of coordination between metal and carboxylic acid groups.

All of our analytical data are consistent with the model that alkaline earth metal ions interact with graphene oxide sheets in two different binding modes (see above), the extent of which depends on the nature of the metal ions themselves. The strongest mode of binding comprises M^{2+} ions tightly bound to carboxylic acid groups at the edges of individual graphene oxide sheets (Figure 4a), resulting in some cross-linking of neighboring sheets and improvements in the mechanical stiffness and strength of the macroscopic paper sample. Additionally, Lewis acidic metal ions such as M^{2+} can induce the ring-opening of epoxides to create C−OH moieties that, together with the already-present carbonyl groups (Figure 4a), then facilitate the intercalation of additional metal ions into the gallery between the graphene oxide sheets and a corresponding increase in *d*-spacing.

The enhanced mechanical stiffness and strength observed for our M-modified graphene oxide paper (see above) is consistent with the chemical model shown in Figure 4. On tensile loading, the edge-bound metal

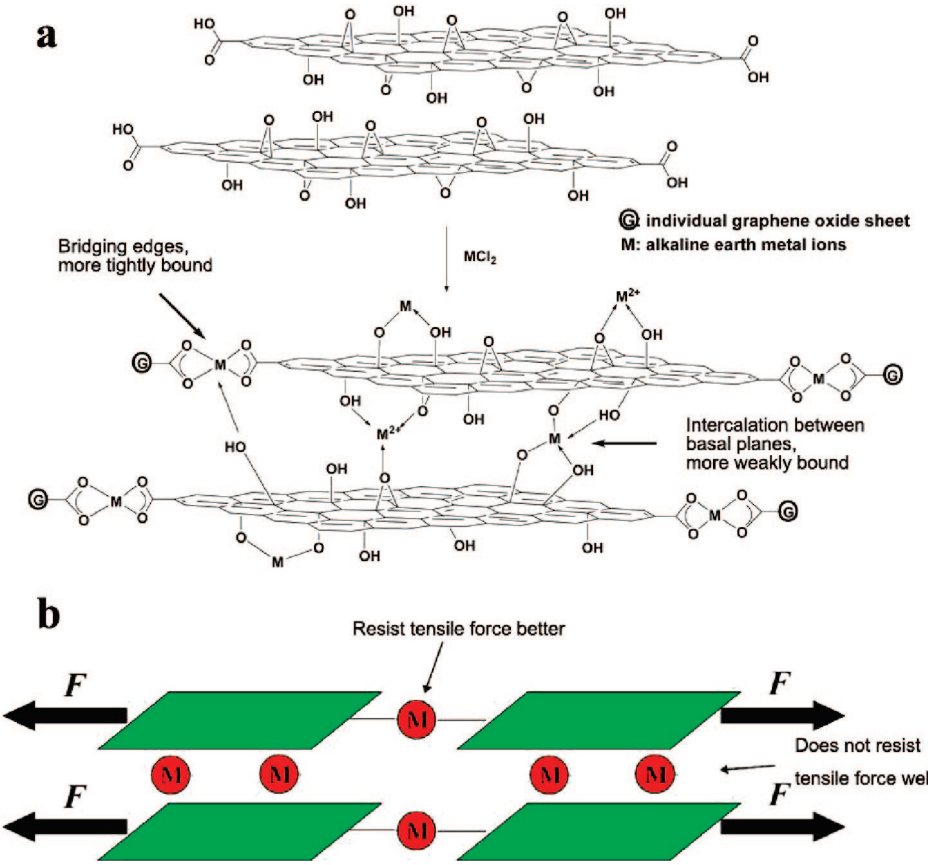

Figure 4. Models of the M-modified graphene oxide papers: (a) schematic model of the reaction between graphene oxide paper and MCl_2 (M = Mg and Ca); (b) proposed model for the enhanced mechanical properties of graphene oxide paper observed after metal modification.

ions, if successfully bridging between carboxylic acid groups on two adjacent graphene oxide sheets, can resist normal deformations between sheets that are on the same plane (Figure 4b). On the other hand, the axial interactions between the metal ions (both edge-bound and intercalated) and the graphene oxide sheets are much weaker and respond to the deformation differently, depending on the magnitude of the loading. During the initial loading, when the force is small, such axial contributions can be significant, resulting in initial moduli that are 70–200% higher than the modulus of unmodified paper. As the specimens enter the straightening regions, where higher tensile force was applied, the relative magnitude of the axial stabilizing contributions diminished and consequently the difference in E_S values between M-modified and unmodified papers are significantly reduced. At this point, the "size" contribution of the intercalated metal ions to the modulus become significant: as metal ions enter the gallery between the graphene oxide sheets in as-prepared M-modified paper, they increase the *d*-spacing and the cross-sectional area of the sample (see SI), leading to an overall reduction of stress (force/cross-sectional area). This phenomenon manifested into a lower E_S for as-prepared Ca-modified paper compared to as-prepared Mg-modified paper (the ionic radius of Ca^{2+} is 1.06 *vs* 0.78 Å for Mg^{2+}).

The macroscopic manifestation of size-dependent negative contribution to the modulus, as described above, becomes most prominent in the "linear region" of the stress–strain curves for both as-prepared M-modified paper samples. Their E_E values now lagged behind that of unmodified paper because of a macroscopic increase in sample thickness that accompanies a reduction in mechanical stress and a negative contribution to the moduli. For the rinsed M-modified samples, where the intercalated metal ions are removed and the *d*-spacings between the sheets are similar to that in the unmodified paper (see ESI), the E_E values do not contain such a negative contribution and are, as mentioned previously, much larger than that of the unmodified samples.

As bonds between alkaline earth metal ions and carboxylate/hydroxyl groups can be reversibly exchanged (with other ions and carboxylate/hydroxyl groups), we hypothesize that repeated cyclic loading of an M-modified paper sample with small force and under slow rate may allow for the galleries in that sample to chemically "anneal" to the best structure. In other words, if small mechanical perturbations can cause the

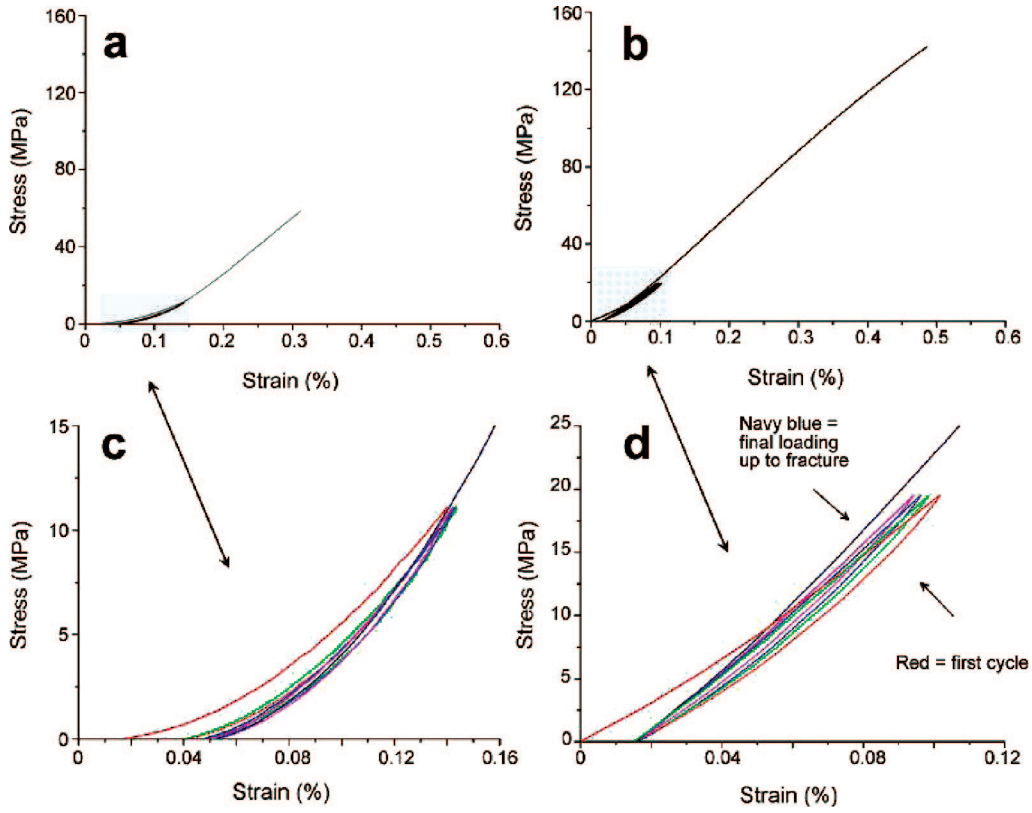

Figure 5. Stress–strain curves obtained for the graphene oxide papers in cyclic loading experiments: (a) full plots for unmodified graphene oxide paper; (c) magnified initial region during cyclic loading experiments; (b) full plots for rinsed Ca-modified graphene oxide paper; (d) magnified initial region during cyclic loading experiments. (Red, first loading; green, second loading; blue, third loading; purple, fourth loading; and navy blue, fifth loading up to fracture.)

edge-bound metal ions to adopt more favorable chemical interactions with the oxygen functionalities of graphene oxide sheets, the stiffness and strength in the M-modified graphene oxide papers would be enhanced. This is indeed the case. After four cycles of loading/unloading (0.001 to 0.5 N and back at 0.005 N/min), the moduli E_E and tensile strength of the M-modified graphene oxide papers, both as-prepared and rinsed, were higher (10–40% higher for modulus and 10–80% for tensile strength) than that of the nonannealed samples (see SI). This is in stark contrast to the behavior of the unmodified graphene oxide paper samples, which exhibited similar moduli, with or without cyclic loading. The magnified stress–strain curve of the rinsed Ca-modified graphene oxide sample under cyclic loading experiment (Figure 5c,d) showed consecutive enhancement of modulus as the number of loading/unloading cycles increased. In comparison, the stress–strain curve of the unmodified paper did not change significantly over the same number of cycles. The overall result is a relative 40–130% enhancement in strength for "mechanically annealed" (*i.e.*, cyclically loaded) M-modified graphene oxide papers compared to similarly processed unmodified graphene oxide paper.

In conclusion, our modification of graphene oxide paper with alkaline earth metal ions has resulted in significant enhancements in mechanical properties that can be readily understood in terms of fundamental chemical interactions. That a small amount of these divalent metal ions (less than 1 wt %) can increase the modulus and tensile strength of unmodified graphene oxide paper attests to the tremendous increase in properties that simple but specific chemical modifications can bring upon macroscopic materials. We expect that future work on these and other postsynthetic modification strategies for improving the mechanical properties of graphene oxide paper will result in a broad new class of graphene-based materials with enhanced functionalities and properties. Given the intrinsic stiffness and strength expected for both graphene and graphene oxide sheets, it is conceivable that graphene-based materials could ultimately be chemically tuned to be the stiffest and strongest materials (on a per weight basis) that could ever be made. This issue has been discussed in a recent paper on the use of nanoscale materials having very high stiffness/strength to make macroscale structures that manifest the mechanics of their individual nanoscale components.[28]

METHODS

GO was synthesized from purified natural graphite (SP-1, Bay Carbon, MI) by the Hummers method.[9] Colloidal dispersions of individual graphene oxide sheets in water (10 mL of a 3 mg/mL solution) were prepared with the aid of ultrasound (Fisher Scientific FS60 ultrasonic cleaning bath) in 20-mL batches. Unmodified graphene oxide paper was made by filtration of the resulting colloid through an Anodisc membrane filter (47 mm in diameter, 0.2-μm pore size, Whatman, Middlesex, U.K.), followed by addition of aqueous MCl_2 solution (10 mL of 0.2-mM solutions, M = Mg and Ca; $BaCl_2$ was not examined owing to its reaction with the membrane) to the wet, unmodified graphene oxide paper. After the filtration, the as-prepared M-modified graphene oxide paper was suction-dried for 1 day, then air-dried for 1–2 days, before being peeled from the filter. To prepare the rinsed M-modified graphene oxide papers, nanopure water (18.2 MΩ resistance, 3 $\times$ 10 mL) was passed through the wet M-modified paper prior to suction-drying, air drying, and peeling from the filter.

Static mechanical uniaxial in-plane tensile tests were conducted with a dynamic mechanical analyzer (2980 DMA, TA Instruments, New Castle, DE). The samples were mounted using film tension clamps with a clamp compliance of *ca.* 0.2 μm/N. The sample width was measured using standard calipers (Mitutoyo Co., Japan). The length between the clamps was measured by the DMA instrument, and the sample thickness was obtained from SEM imaging of the fracture edge. Normal tensile tests were initially conducted for 4 h at 35 °C in controlled-force mode with a preload of 0.01 N, and force was loaded with a force ramp rate of 0.05 N/min. The cyclic tensile tests were carried out with a preload of 0.001 N for 4 h at 35 °C, a loaded force of 0.5 N, and force ramp rate of 0.005 N/min for four cycles, followed by loading up to fracture with a force ramp rate of 0.05 N/min. XPS measurements were performed using an Omicron ESCA Probe (Omicron Nanotechnology, Taunusstein, Germany) with a monochromated Al Kα radiation ($h\nu$ = 1486.6 eV).

Acknowledgment. We appreciate support from NASA through the University Research, Engineering, and Technology Institute (URETI) on Bioinspired Materials (BiMat), from DARPA (iMINT), and from the National Science Foundation. S.P. was partially supported by a Korea Research Foundation Grant funded by the Korean Government (MOEHRD) (KRF-2006-352-C00055). Gulay Bozoklu is supported by I2CAM NSF Grant No. DMR0645461. This work made use of X-ray facilities supported by the MRSEC program of the National Science Foundation at the Materials Research Center of Northwestern University, and ICP−MS facilities at the Korean Research Institute of Standard and Science (KRISS) supported by the Korean government. We thank I. M. Daniel for the use of his mechanical testing instruments and Jeong-Min Cho for helpful discussions. Both I. M. Daniel and A. L. Ruoff provided a critical reading of an initial draft of this manuscript.

Supporting Information Available: Materials and methods; DMA, SEM, ICP-MS, EDX, XRD, XPS, FT-IR, and Raman data. This material is available free of charge *via* the Internet at http://pubs.acs.org.

REFERENCES AND NOTES

1. Geim, A. K.; Novoselov, K. S. The Rise of Graphene. *Nat. Mater.* **2007**, *6*, 183–191.
2. Wu, J.; Pisula, W.; Mullen, K. Graphenes as Potential Material for Electronics. *Chem. Rev.* **2007**, *107*, 718–747.
3. Novoselov, K. S.; Geim, A. K.; Morozov, S. V.; Jiang, D.; Zhang, Y.; Dubonos, S. V.; Grigorieva, I. V.; Firsov, A. A. Electric Field Effect in Atomically Thin Carbon Films. *Science* **2004**, *306*, 666–669.
4. Novoselov, K. S.; Geim, A. K.; Morozov, S. V.; Jiang, D.; Katsnelson, M. I.; Dubonos, S. V.; Firsov, A. A. Two-dimensional Gas of Massless Dirac Fermions in Graphene. *Nature* **2005**, *438*, 197–200.
5. Brink, J. v. d. From Strength to Strength. *Nat. Nanotechnol.* **2007**, *2*, 199–201.
6. Zhang, Y.; Tan, Y.-W.; Stormer, H. L.; Kim, P. Experimental Observation of the Quantum Hall Effect and Berry's Phase in Graphene. *Nature* **2005**, *438*, 201–204.
7. Pereira, J. M.; Vasilopoulos, P.; Peeters, F. M. Tunable Quantum Dots in Bilayer Graphene. *Nano Lett.* **2007**, *7*, 946–949.
8. White, C. T.; Li, J.; Gunlycke, D.; Mintmire, J. W. Hidden One-Electron Interactions in Carbon Nanotubes Revealed in Graphene Nanostrips. *Nano Lett.* **2007**, *7*, 825–830.
9. Hummers, W. S.; Offeman, R. E. Preparation of Graphitic Oxide. *J. Am. Chem. Soc.* **1958**, *80*, 1339.
10. He, H.; Klinowski, J.; Forster, M.; Lerf, A. A New tSructural Model for Graphite Oxide. *Chem. Phys. Lett.* **1998**, *287*, 53–56.
11. He, H.; Riedl, T.; Lerf, A.; Klinowski, J. Solid-state NMR Studies of the Structure of Graphite Oxide. *J. Phys. Chem.* **1996**, *100*, 19954–1995.
12. Lerf, A.; He, H.; Forster, M.; Klinowski, J. Structure of Graphite Oxide Revisited. *J. Phys. Chem. B* **1998**, *102*, 4477–4482.
13. Lerf, A.; He, H.; Riedl, T.; Klinowski, J. ^{13}C and ^{1}H MAS NMR Studies of Graphite Oxide and Its Chemically Modified Derivatives. *Solid State Ionics* **1997**, *101–103*, 857–862.
14. Stankovich, S.; Piner, R.; Chen, X.; Wu, N.; Nguyen, S. T.; Ruoff, R. S. Stable Aqueous Dispersions of Graphitic Nanoplatelets *via* the Reduction of Exfoliated Graphite Oxide in the Presence of Poly(sodium 4-styrenesulfonate). *J. Mater. Chem.* **2006**, *16*, 155–158.
15. Stankovich, S.; Piner, R.; Nguyen, S. T.; Ruoff, R. S. Synthesis and Exfoliation of Isocyanate-treated Graphene Oxide Nanoplatelets. *Carbon* **2006**, *44*, 3342–3347.
16. Stankovich, S.; Dikin, D. A.; Dommett, G. H. B.; Kohlhaas, K. M.; Zimney, E. J.; Stach, E. A.; Piner, R.; Nguyen, S. T.; Ruoff, R. S. Graphene-based Composite Materials. *Nature* **2006**, *442*, 282–286.
17. Stankovich, S.; Dikin, D. A.; Piner, R.; Kohlhaas, K. M.; Kleinhammes, A.; Jia, Y.; Wu, Y.; Nguyen, S. T.; Ruoff, R. S. Synthesis of Graphene-based Nanosheets *via* Chemical Reduction of Exfoliated Graphite Oxide. *Carbon* **2007**, *45*, 1558–1565.
18. Watcharotone, S.; Dikin, D. A.; Stankovich, S.; Piner, R.; Jung, I.; Dommett, G. H. B.; Evmenenko, G.; Wu, S. E.; Chen, S. F.; Liu, C. P.; Nguyen, S. T.; Ruoff, R. S. Graphene-Silica Composite Thin Films as Transparent Conductors. *Nano Lett.* **2007**, *7*, 1888–1892.
19. Dikin, D. A.; Stankovich, S.; Zimney, E. J.; Piner, R.; Dommett, G. H. B.; Evmenenko, G.; Nguyen, S. T.; Ruoff, R. S. Preparation and Characterization of Graphene Oxide Paper. *Nature* **2007**, *448*, 457–460.
20. Zhang, X. F.; Sreekumar, T. V.; Liu, T; Kumar, S. Properties and Structure of Nitric Acid Oxidizied Single Wall Carbon Nanotube Films. *J. Phys. Chem. B* **2004**, *108*, 16435–16440.
21. Dowell, M. B.; Howard, R. A. Tensile and Compressive Properties of Flexible Graphite Foils. *Carbon* **1986**, *24*, 311–323.
22. Ballard, D. G. H.; Rideal, G. R. Flexible Inorganic Films and Coatings. *J. Mater. Sci.* **1983**, *18*, 545–561.
23. Lerf, A.; Buchsteiner, A.; Pieper, A.; Schotti, S.; Dekany, I.; Szabo, T.; Boehm, H. P. Hydration Behavior and Dynamics of Water Molecules in Graphite Oxide. *Carbon* **2006**, *67*, 1106–1110.
24. Emsley, J. *The Elements*; Clarendon Press: Oxford, 1989; pp 40 and 108..
25. Lambert, J. B.; Shurvell, H. F.; Lightner, D. A.; Cooks, R. G. *Organic Structural Spectroscopy,* 2nd ed.; Prentice Hall: New York, 2001; pp 189–196..
26. Nakamoto, K. *Infrared and Raman Spectra of Inorganic and Coordination Compounds,* 4th ed.; John Wiley & Sons: New York, 1986; pp. 231–233..
27. Moulder, J. F.; Stickle, W. F.; Sobol, P. E.; Bomben, K. D. *Handbook of X-ray Photoelectron Spectroscopy*; Physical Electronics, Inc.: Eden Prairie, MN, 1995; pp 216–217..
28. Hamsa, P. K.; Turner, P. J.; Ruoff, R. S. Optimized Adhesives for Strong Lightweight, Damage-Resistant, Nanocomposite Materials: New Insights from Natural Materials. *Nanotechnology* **2007**, *18*, 044026.